Available online at www.sciencedirect.com
SCIENCE DIRECT
Talanta 69 (2006) 1240–1245
Talanta
www.elsevier.com/locate/talanta

Probing chiral amino acids at sub-picomolar level based on bovine serum albumin enantioselective films coupled with silver-enhanced gold nanoparticles

Yunxia Wang, Xiuli Yin, Mianhong Shi, Wei Li, Lei Zhang, Jilie Kong *

Department of Chemistry, Fudan University, Shanghai 200433, PR China

Received 24 September 2005; received in revised form 26 December 2005; accepted 26 December 2005
Available online 18 April 2006

Abstract

A novel electrochemical sensor with capability of probing chiral amino acids with gold nanoparticle (n-Au) labels using bovine serum albumin (BSA) as a chiral selector and subsequent signal amplification step by silver enhancement is introduced. The assay relies on the stereoselectivity of BSA embedded in ultrathin γ-alumina sol–gel film coated on the surface of the glassy carbon electrode (GCE). The recognition to the n-Au-labeled L- or D-amino acids for BSA-GCE could be monitored by the differential pulse voltammetry (DPV), while the DPV signal was greatly amplified by the anchored silver atoms on the n-Au, leading to a new way of quantitatively analysis of chiral amino acids electrochemically at sub-picomolar level. With L-tryptophan as the probe solute, the linear concentration range was from 1.33×10^{-12} to 1×10^{-9} mol L^{-1} and detection limit was 5×10^{-13} mol L^{-1}. For tryptophan enantiomers, the enantioselectivity coefficient 2.3 was obtained.

Keywords: Electrochemical sensor; Chiral recognition; Bovine serum albumin (BSA); Chiral amino acids; Gold nanoparticles; Silver enhancement

1. Introduction

Chirality is a determinative property of most biological molecules, and the development of refined analytical techniques for the precise determination of bioactive chiral molecules is of great interest. Up to now, various sensor technologies have been developed for chiral compounds, and chiral selectors for enantiomer discrimination have largely built upon empiric chromatographic phases [1–3]. It has been proven that the protein-chiral stationary phase usually results in better enantiomer discrimination in general because proteins possess complex and changeable conformations. Take BSA as an example, it has been demonstrated to be useful in separating the optical isomers of drugs, small molecules and especially amino acids [4–6], thereby, indicating the probable utility of such selectivity in electrochemical chiral analysis, provided appropriate electrochemical system is proposed. However, BSA has not been used as a chiral selector in electrochemical chiral discrimination as far as we know. Thus, developing chiral sensor based on the stereoselectivity of BSA motivated our group to undertake this work.

The first crucial issue for the BSA sensor is the attachment method of BSA onto electrodes. The covalent binding technique was often used for the functional protein immobilization because it could bind the target artificially to form an ordered and dense monolayer [7,8], however, the covalent immobilization process of the protein on the electrode surface was somewhat complex, and the procedure might denature the protein [9]. In recent years, the use of sol–gel chemistry to encapsulate the proteins has been reported as an alternative effective method applied to immobilization of protein. Compared with the covalent binding technique, the low-temperature sol–gel technique possesses advantages for embedding the biological macromolecules because it could, not only provide mild chemical conditions for preserving the integrity and homogeneity of the protein surface microstructure [10,11], but also make the biological macromolecules move freely in the holes of the sol–gel matrix [12]. Therefore, it is promising to incorporate γ-alumina sol–gel in sensor for protein immobilization.

* Corresponding author. Tel.: +86 21 65642138; fax: +86 21 65641740.
E-mail address: jlkong@fudan.edu.cn (J. Kong).

0039-9140/$ – see front matter © 2006 Elsevier B.V. All rights reserved.
doi:10.1016/j.talanta.2005.12.060

On the other hand, nanoparticle-based materials offer excellent prospects for chemical and biological sensing [13,14]. It has been reported that amino acids could be labeled by n-Au in aqueous phase by the strong electrostatic interaction between amino group and the n-Au, and such characteristics provided n-Au-labeled amino acids with immediate biological applications such as bio-labeling and drug delivery [15]. In addition, silver deposition on n-Au based on n-Au-promoted reduction of silver(I) is commonly used in DNA detection and immunoreaction for sensitivity improvement [16–18]. Therefore, such method of silver-enhanced colloid gold may hold great potential for the detection of amino acids with n-Au labels.

In the present work, chiral analysis of n-Au-labeled amino acid isomers based on BSA stereoselectivity was demonstrated. n-Au-labeled amino acid enantiomers were selectively bound by BSA on the surface of the GCE. After silver enhancement, the voltammetric signals of silver atoms were detected by electrochemical DPV. As far as we know, it is the first time for BSA to be used in electrochemical chiral recognition. The influence of various factors including phosphate buffer pH, incubation time and silver deposition time on the chiral recognition response was investigated, and electrochemical impedance spectroscopy (EIS) was also used to characterize the chiral recognition phenomena of BSA.

2. Experimental

2.1. Chemicals and materials

Bovine serum albumin (BSA, fraction V) was obtained from Sino-American Biotechnology Co. (Shanghai, China). D-/L-Tryptophan (D-/L-Trp), D-/L-phenylalanine, D-/L-tyrosine, D-/L-lysine and D-/L-proline were purchased from Sigma–Aldrich (Milwaukee, WI). $HAuCl_4{\cdot}4H_2O$ was purchased from Shanghai Runjie Chemical Reagent Co. (Shanghai, China). All of other chemicals were of analytical grade and used as received. Millipore water was from a Milli-Q synthesis A10 system and used for all solution preparations.

2.2. Preparation and characterization of n-Au

The n-Au was prepared by the conventional reduction protocol [19]. The resulting solution of colloidal nanoparticles was characterized by UV–vis spectroscopy (SM-240 CCD spectrophotometer, CVI Spectral Instruments, Putnam, CT) and transmission electron microscopy (TEM) (JEOL JEM-2011 (Japan), accelerating voltage: 120 kV). Absorption maximum was at 522.2 nm and an average particle size was13 ± 1.5 nm (100 particles sampled).

2.3. Preparation and characterization of n-Au-labeled amino acids enantiomers

The gold nanoparticle-labeled L-tryptophan (n-Au-L-Trp) was prepared by addition of certain volume aqueous solution of 1 mM L-Trp to 9 mL solution of sodium citrate reduced-n-Au, and aging the n-Au solution at room temperature for 2 days. Here L-Trp was taken as a model chiral amino acid and others were prepared and characterized similarly. The obtained solutions were directly used for electrochemical detection. Besides UV–vis spectroscopy and TEM, X-ray photoemission spectroscopy (XPS) (Perkin-Elmer PHI 5000C ESCA system, base pressure: 1×10^{-9} Torr) and ^{1}H NMR (Bruker DMX500-MHz, scan range: 0–15 ppm) were used to explore the characteristics of amino acids labeled by the n-Au.

UV–vis absorption maximum at 525.8 nm and TEM indicating a particle size of 13–15 nm, demonstrated the optical properties and morphology of n-Au after labeling L-Trp had no significant changes. According to XPS measurements of the n-Au-L-Trp, the observed peak of nitrogen (N_{1S}, 400.4 eV) revealed that the n-Au had labeled onto L-Trp [20]. In NMR spectra, n-Au-L-Trp had similar proton signals with pure L-tryptophan except a slight up-field chemical shift of all the protons. These results were in accordance with the literature, further indicating that L-Trp was labeled by the n-Au [15].

2.4. Fabrication of sol–gel-derived thin-film chiral sensors

GCEs ($\Phi = 4$ mm) were polished carefully with alumina slurries (1.0, 0.3 and 0.05 μm) and then cleaned through sonication in Milli-Q water and absolute ethanol. Finally, the electrodes were dried with purified N_2. The sensors were fabricated by dripping the mixture of the BSA (0.1 mg mL^{-1}) and Al_2O_3 sol (prepared as Ref. [10]) (1:1, v/v) 5 μL, with a microliter syringe on bare GCEs. Afterward, the sensors were dried at 4 °C for 3 days.

2.5. Chiral discrimination

At room temperature, the modified electrodes were separately incubated in 10 mL of 10 mM phosphate buffer solutions of the n-Au labeled Trp enantiomers with the same concentration for certain time, then the electrodes were washed with copious Milli-Q water to remove the physically absorbed n-Au-labeled Trp enantiomers.

2.6. Silver enhancement of n-Au

After the chiral discrimination reaction, n-Au-L-Trp/BSA and n-Au-D-Trp/BSA electrodes were incubated in the silver enhancer solution (150 μL 0.22% aqueous silver nitrate and 150 μL 1% hydroquinone in aqueous 0.55 mol L^{-1} sodium citrate buffer, pH 3.8) for certain time, and then in 2.5% sodium thiosulfate pentahydrate for 3 min, finally the electrodes were thoroughly washed with Milli-Q water.

Note: The silver enhancement solution was prepared immediately before application and the above procedure was carried out in dark room.

2.7. Electrochemical DPV measurement

Electrochemical DPV measurements were performed at room temperature in a 10 mL electrochemical cell with a normal three-electrode configuration consists of the saturated calomel

reference electrode (SCE), the platinum wire counter electrode and the working electrode after chiral discrimination and silver enhancement, the reference electrode was separated from the working solution by a double electrolytic salt bridge filled with saturated KNO_3 in order to avoid determination interfere caused by the continuous leaching of chloride anion that lead to AgCl precipitation. DPV determination of deposited silver was performed in 0.1 mol L^{-1} HAc–NaAc buffers (pH 5.2). The DPV scan was ranged from +0.10 to +0.80 V (versus SCE).

2.8. Electrochemical impedance spectroscopy characterization

Faradic impedance measurements were carried out with Potentiostat/Galvanostat Model 273A and Model 5210 Lock-In Amplifier. The experiments were performed in 10 mL aqueous solution containing 0.1 M KCl and 0.01 M $K_3[Fe(CN)_6]/K_4[Fe(CN)_6]$ (1:1) mixture as a redox probe. Impedance measurements were performed in the frequency range from 1×10^5 to 0.01 Hz at a sampling rate of 12 point per decade (AC amplitude: 5 mV) and the impedance spectra were plotted in the form of complex plane diagrams (Nyquist plots, Z_{im} versus Z_{re}).

3. Results and discussion

3.1. BSA electrochemical recognition of chiral amino acids

The whole process of the electrochemical recognition of chiral amino acids is depicted in Scheme 1. In this work, 'silver enhancement' technology was used to amplify the voltammetric signals of n-Au labeled amino acids selectively trapped by BSA via DPV measuring of the deposited silver. Fig. 1a and b shows DPV curves of silver obtained by the chiral sensors under the optimum conditions after respective reaction with n-Au-L-Trp (Fig. 1a) and n-Au-D-Trp (Fig. 1b), and subsequently silver enhancement. A well-shaped anodic peak of silver centered at

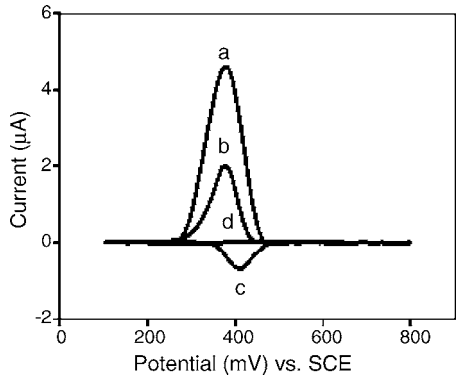

Fig. 1. DPV responses of silver for n-Au-L-Trp (a) and n-Au-D-Trp (b) on the chiral sensors after silver enhancement, direct DPV responses of gold for n-Au-L-Trp (c) and n-Au-D-Trp (d) on the sensors, free of silver enhancement. Potential range: +0.10 to +0.80 V (vs. SCE); pulse amplitude: 50 mV; pulse width: 50 ms; pulse period: 0.2 s (a and b); oxidation of gold labels: +1.25 V, 150 s; reversed scanning potential: +0.65 to +0.15 V (vs. SCE) (c and d).

+ 0.38 V (versus SCE) was obtained [21], and the DPV peak current of silver for n-Au-L-Trp (Fig. 1a) is ~2.3 times greater than that for n-Au-D-Trp (Fig. 1b). The remarkable difference of the DPV peak currents between n-Au-L-Trp and n-Au-D-Trp indicated that the BSA sensor had stereoselectivity towards Trp enantiomers and had bound more L-Trp than D-Trp. These results agree well with the fact that L-Trp binds more strongly to BSA than D-Trp does in chiral chromatography separation [4–6]. Therefore, recognition of chiral amino acids by anchored BSA was successfully achieved via electrochemical measurement.

Meanwhile, the control DPV response of gold was also explored to investigate the silver enhancement strategy. Fig. 1c and d gives the optimized DPV response of gold for the chiral sensors after separate reaction with n-Au-L-Trp (Fig. 1c) and with n-Au-D-Trp (Fig. 1d), free of silver enhancement. The DPV measurement was performed in 0.1 M HCl solution by applying +1.25 V (versus SCE) for 150 s, then immediately running reversed scanning from +0.65 to +0.15 V. The peak current of gold located at +0.40 V was taken as analytical response [20].

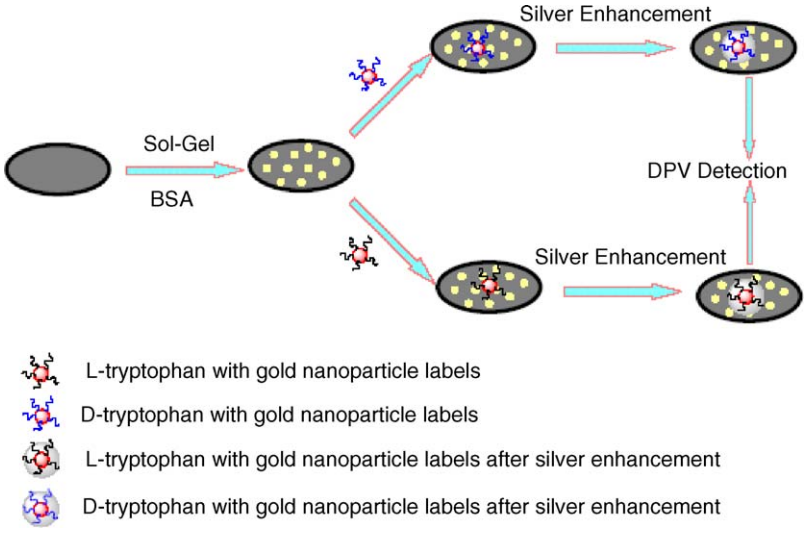

Scheme 1. Process summary of BSA electrochemical recognition of chiral amino acids based on silver-enhanced n-Au labels.

By comparison between Fig. 1a and c, it can be observed that voltammetric signal of silver for n-Au-L-Trp (Fig. 1a) is about seven times greater than that of bare gold tags (Fig. 1c) (4.61 μA versus 0.69 μA), which indicated the higher sensitivity of the silver enhancement strategy and provided the possibility for the sensor to obtain a lower detection limit. Besides, the normally used media, i.e. 0.1 M HCl, for the direct n-Au detection was not desirable for the chiral discrimination of protein, because the protein should be denatured [22], whereas the electrochemical detection for silver shell protected n-Au was carried out in the pH 5.2 acetate buffer solutions which had no influence on protein and the chiral discrimination.

In order to demonstrate the selectivity of the chiral sensor, the enantioselectivity of the chiral sensor was evaluated quantitatively using enantioselectivity coefficient α, analogous to separation efficiency in chromatography [4], which is defined as the following equation:

$$\alpha = \frac{I_{p_L}}{I_{p_D}}$$

where I_{p_L} and I_{p_D} are the averaged anodic peak currents of silver corresponding to L- and D-amino acid with n-Au tags after silver deposition under the same conditions. The chiral selectivity of BSA-GCE to n-Au-Trp enantiomers was investigated by varying the tryptophan enantiomer concentration in electrochemical detection over the range of 1.33×10^{-13} to 1×10^{-6} mol L^{-1}. Fig. 2 shows the responses of the oxidation peak currents of silver (R.S.D., $n = 3$) and the enantioselectivity coefficient (R.S.D., $n = 3$) to tryptophan enantiomer concentration. As shown in Fig. 2, the oxidation peak currents for L- and D-tryptophan exhibited sectionalized linear responses in the concentration range of 1.33×10^{-12} to 1×10^{-9} and 1.33×10^{-12} to 5×10^{-12} mol L^{-1}, with the regressing equation $Y = 11.93 + (0.8746 \times 10^{10})X$ ($R = 0.9923$) and $Y = 5.878 + (0.3654 \times 10^{10})X$ ($R = 0.9773$), respectively. These results illustrated that the interactions between BSA and Trp enantiomers had much difference. The same detect limit 5×10^{-13} mol L^{-1} was obtained for the Trp enantiomers (the detection limit was estimated using 3σ, σ is the standard deviation of a blank response, $n = 11$), which was one or two magnitudes lower than those of currently reported enantioselective membrane electrodes [23,24], and further showed the superior sensitivity of the silver enhancement strategy. As for enantioselectivity, the enantioselectivity coefficient α 1.03 was obtained when tryptophan enantiomer concentration was 1.33×10^{-13} mol L^{-1}, and α continuously increased with the rise of the tryptophan enantiomer concentration, eventually the maximum α (2.3) was achieved. These revealed that the chiral sensor was highly stereoselective and extremely sensitive via the using of BSA as chiral selector and the employment of silver enhancement of n-Au labels coupled with electrochemical DPV detection.

To further explore the reliability of the chiral sensor, other five amino acids, phenylalanine, tyrosine, proline, alanine and lysine, were also examined by the sensor under the same labeling and detecting conditions as that for tryptophan. Among these five amino acids, phenylalanine and tyrosine were found to be discriminated with α of 1.30 and 1.36, respectively, while the rest three were not, which is presumed to be due to stronger hydrophobicity for the former two and the weaker hydrophobicity for the latter three amino acids, considering the fact that the enantiomeric selectivity of BSA was mainly based on the steric, hydrophobic and hydrogen-bonding interactions [6]. The observed selectivity towards the two amino acids further verified the efficiency of this chiral sensor.

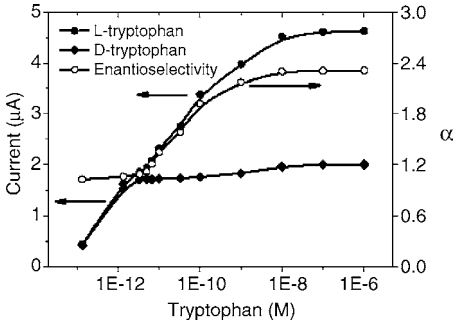

Fig. 2. Responses of the DPV peak currents and enantioselectivity coefficient α to the concentration of Trp enantiomers.

3.2. Electrochemical impedance spectroscopy characterization

EIS technique was used to characterize the chiral discrimination since the electrode immobilized with BSA after reaction with the n-Au-Trp enantiomers and subsequently silver deposition would result in the increase of interfacial electron transfer resistance (R_{et}), and thus the chiral recognition of BSA can be visualized by the change of R_{et} [25]. Fig. 3 illustrates the results of the Faradic impedance detection of the chiral recognition. As can be seen from Fig. 3, the semicircle diameter kept on increasing from BSA-GCE (Fig. 3a), to BSA-GCEs separately incubated with n-Au-D-Trp (Fig. 3b), n-Au-L-Trp (Fig. 3c) and subsequent silver enhancement. By simulating the results with the corresponding equivalent circuit (I) (for a) and (II) (for b and c), the obtained R_{et}s for a, b and c were 119.7, 23,273 and

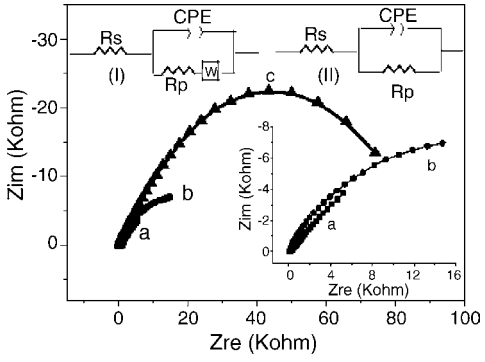

Fig. 3. Nyquist diagram (Z_{im} vs. Z_{re}) for the Faradic impedance of BSA immobilized GCE (a), BSA immobilized GCE after chiral discrimination reaction with n-Au-D-Trp (b) and n-Au-L-Trp (c) and subsequent silver enhancement. *Inset*: Equivalent circuits (I) and (II) corresponding to the impedance features of (a) and (b and c), respectively.

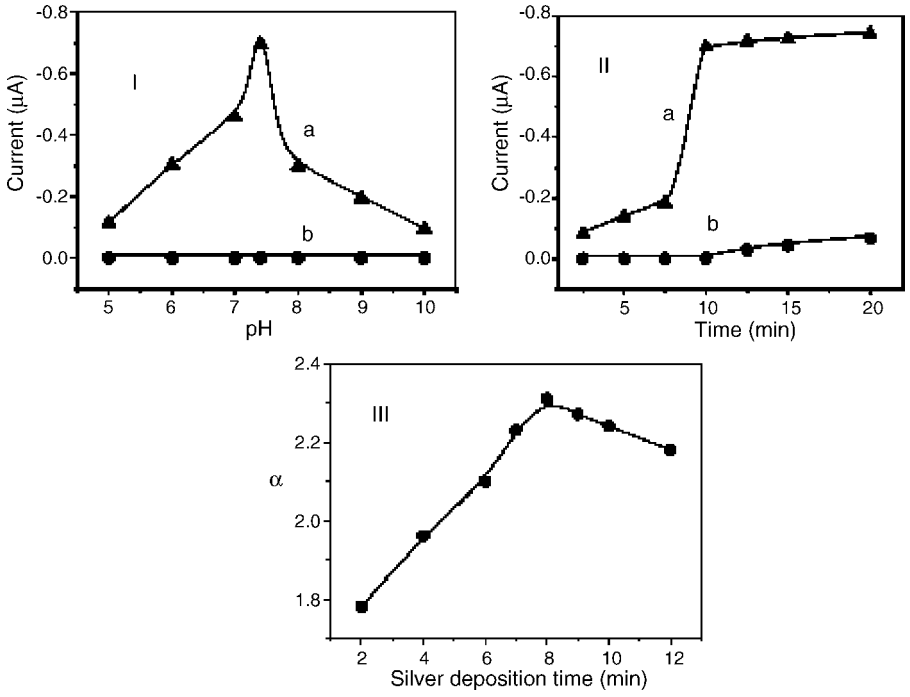

Fig. 4. Optimization of the chiral recognition conditions: pH of phosphate buffer for incubation (I), incubation time (II) and silver deposition time (III) for n-Au-L-Trp (a) and n-Au-D-Trp (b).

73,349 Ω, respectively, which clearly indicated that BSA had bound much more n-Au-L-Trp than n-Au-D-Trp. The results were well consistent with that of the electrochemical DPV detection.

3.3. Optimization of chiral discrimination conditions

3.3.1. pH of phosphate buffer for incubation

It is well known in chromatography that phosphate buffer pH plays an important role in enantiospecificity of amino acid bound by BSA [5]. In this work, the optimization was performed in the pH range of 5–10, and ultimately DPV detection of gold tags (depicted in Fig. 4I). The peak current of gold tags for n-Au-D-Trp (Fig. 4I(b)) was almost constant 0 in the pH range of 5–10, while in the pH range of 5–7.4, the peak current of gold tags for n-Au-L-Trp (Fig. 4I(a)) was increased along with the increasing of the pH, and an inversed peak current change was observed in the following pH 7.4–10, which indicated the buffer of pH 7.4 was appropriate to the chiral recognition. The obtained tendency of chiral recognition with pH may be derived from the fact that BSA is composed of three globular domains and maintains the most compact configuration at physiological pH, and either increasing the pH of the medium to 10 or decreasing it to 5, resulted in the change of the favored globular configuration, further influenced BSA binding of the amino acids [22].

3.3.2. Incubation time

The effect of the incubation time on chiral discrimination was also explored. The incubation time was varied from 2.5 to 20 min. As shown in Fig. 4II, with the reaction time increased, the peak current of n-Au-D-Trp (Fig. 4II(b)) was constant 0 during 2.5–10 min, and after that, it increased very slowly. As for n-Au-L-Trp (Fig. 4II(a)), the peak current rose gradually at first (up to 10 min) and then increased very slowly, suggesting that up to 10 min, the interaction of BSA and n-Au-Trp enantiomers had reached saturation, and the continuous peak current increase with increased time was due to the fact that physically absorbed amount of n-Au-Trp enantiomers also increased, thus the selectivity would drop on the contrary. Taking account of the selectivity and sensitivity, 10 min was employed as the incubation time.

3.3.3. Silver deposition time

The ultimate objective of the silver enhancement in this work is to control the catalytic deposition of silver on n-Au, while avoiding spontaneously deposition onto other components of the system, because an excess of silver can enhance the blank signals and further affect the reliability of the DPV signal. Here this blank signal was eliminated by adding a sodium thiosulfate fixer solution (that transfers the silver cation into the $Ag(S_2O_3)_3^{5-}$ anion) and by controlling the silver deposition time. Fig. 4III shows the effect of the silver deposition time on the enantioselectivity of the sensor. The silver enhancement time was changed in the range of 2–12 min. As depicted in Fig. 4III, the enantioselective coefficient increased linearly with the deposition time over the range of 2–8 min, then dropped slowly with continuously increased silver deposition time, which suggested that an excess of silver had appeared and affected the selectivity. Considering that precipitation periods no longer than 8 min assured that only the n-Au labels were coated with silver and 8 min just offered the best trade-off between high sensitivity and selectivity, 8 min time was chosen for silver accumulation [17].

4. Conclusions

A novel chiral sensor based on BSA's stereoselectivity has been established to discriminate n-Au-labeled chiral amino acids. As far as we know, it is the first time for anchored BSA to achieve chiral recognition electrochemically. Coupled with the considerable signal amplification advantage of the silver-enhanced colloidal gold in DPV measurement, the chiral sensor provided efficient recognition to tryptophan, phenylaniline and tyrosine enantiomers. The introduction of BSA in electrochemical chiral analysis represents an attractive addition to the arsenal of electrochemical enantioselective measurement, and the analytical formats could also be applicable to affinity assays, molecular recognition and microanalysis.

Acknowledgements

This work was supported by NSFC (20335040, 20475012, 20525519), 973 (2001CB510202), Shanghai nano project (0452 nm 003) and TRAPOYT.

References

[1] A. Tsourkas, O. Hofstetter, H. Hofstetter, R. Weissleder, L. Josephson, Angew. Chem. Int. Ed. 43 (2004) 2395.
[2] A. Ghanem, Talanta 66 (2005) 1234.
[3] K. Bodenhofer, A. Hierlemann, J. Seemann, G. Gauglitz, B. Koppenhoefer, W. Gopel, Nature 387 (1997) 577.
[4] M. Kato, K. Sakai-Kato, N. Matsumoto, T. Toyo'oka, Anal. Chem. 74 (2002) 1915.
[5] M. Kato, N. Matsumoto, K. Sakai-Kato, T. Toyo'oka, J. Pharm. Biomed. 30 (2003) 1845.
[6] C.V. Kumar, A. Buranaprapuk, H.C. Sze, Chem. Commun. 3 (2001) 297.
[7] E. Katz, L. Alfonta, I. Willner, Sens. Actuators B 76 (2001) 134.
[8] X.Q. Zhang, V. Deckert, B. Steiger, M.K.N. Hirayama, U.W. Suter, E. Pretsch, Talanta 63 (2004) 159.
[9] W. Jin, J.D. Rennan, Anal. Chim. Acta 461 (2002) 1.
[10] D.C. Jiang, J. Tang, B.H. Liu, P.Y. Yang, J.L. Kong, Anal. Chem. 75 (2003) 4578.
[11] M.H. Shi, J.J. Xu, S. Zhang, B.H. Liu, J.L. Kong, Talanta 68 (2006) 1047.
[12] X.B. Zuo, K.M. Wang, L.J. Zhou, S.S. Huang, Electrophoresis 24 (2003) 3202.
[13] B. Dubertret, M. Calame, A.J. Libchaber, Nat. Biotechnol. 19 (2001) 365.
[14] W. Vastarella, R. Nicastri, Talanta 66 (2005) 627.
[15] P. Selvakannan, S. Mandal, S. Phadtare, A. Gole, R. Pasricha, S.D. Adyanthaya, M. Sastry, J. Colloid Interface Sci. 269 (2004) 97.
[16] H.S. Guo, N.Y. He, S.X. Ge, D. Yang, J.N. Zhang, Talanta 68 (2005) 61.
[17] J. Wang, R. Polsky, D. Xu, Langmuir 17 (2001) 5739.
[18] T.A. Taton, C.A. Mirkin, R.L. Letsinger, Science 289 (2000) 1757.
[19] K.C. Grabar, R.G. Freeman, M.B. Hommer, M.J. Natan, Anal. Chem. 67 (1995) 735.
[20] H. Joshi, P.S. Shirude, V. Bansal, K.N. Ganesh, M. Sastry, J. Phys. Chem. B 108 (2004) 11535.
[21] H. Cai, Y.Q. Wang, P.G. He, Y.Z. Fang, Anal. Chim. Acta 469 (2002) 165.
[22] T.O. Hushcha, A.I. Luik, Y.N. Naboka, Talanta 53 (2000) 29.
[23] Y.X. Zhou, B. Yu, K. Levon, Chem. Mater. 15 (2003) 2774.
[24] K.I. Ozoemena, R.L. Stefan, Sens. Actuators B 98 (2004) 97.
[25] Y. Xu, H. Cai, P.G. He, Y.Z. Fang, Electroanalysis 16 (2004) 150.